

1                   **Neonatal hyperoxia enhances age-dependent expression**  
2                   **of SARS-CoV-2 receptors in mice**

3  
4                   Min Yee<sup>1</sup>  
5                   E. David Cohen<sup>1</sup>  
6                   Jeannie Haak<sup>1</sup>  
7                   Andrew M. Dylag<sup>1</sup>  
8                   Michael A. O'Reilly<sup>1,2</sup>

9  
10                  The Department of Pediatrics  
11                  School of Medicine and Dentistry,  
12                  The University of Rochester,  
13                  Rochester, NY 14642

14  
15  
16  
17                  <sup>2</sup>**Address Correspondence to:**

18  
19                  Michael A. O'Reilly, Ph.D.  
20                  Department of Pediatrics  
21                  Box 850  
22                  The University of Rochester  
23                  School of Medicine and Dentistry  
24                  601 Elmwood Avenue  
25                  Rochester NY 14642  
26                  Tel: (585) 275-5948  
27                  Fax: (585) 756-7780  
28                  Email: michael\_oreilly@urmc.rochester.edu

29  
30  
31                  **Running Title:** Modifiers of SARS-CoV-2 receptor expression  
32  
33

34 **ABSTRACT**

35           The severity of COVID-19 lung disease is higher in the elderly and people with pre-existing co-  
36 morbidity. People who were born preterm may be at greater risk for COVID-19 because their early  
37 exposure to oxygen at birth increases their risk of being hospitalized when infected with RSV and  
38 other respiratory viruses. Our prior studies in mice showed how high levels of oxygen (hyperoxia)  
39 between postnatal days 0-4 increases the severity of influenza A virus infections by reducing the  
40 number of alveolar epithelial type 2 (AT2) cells. Because AT2 cells express the SARS-CoV-2  
41 receptors angiotensin converting enzyme (ACE2) and transmembrane protease/serine subfamily  
42 member 2 (TMPRSS2), we expected their expression would decline as AT2 cells were depleted by  
43 hyperoxia. Instead, we made the surprising discovery that expression of *Ace2* and *Tmprss2* mRNA  
44 increases as mice age and is accelerated by exposing mice to neonatal hyperoxia. ACE2 is primarily  
45 expressed at birth by airway Club cells and becomes detectable in AT2 cells by one year of life.  
46 Neonatal hyperoxia increases ACE2 expression in Club cells and makes it detectable in 2-month-old  
47 AT2 cells. This early and increased expression of SARS-CoV-2 receptors was not seen in adult mice  
48 who had been administered the mitochondrial superoxide scavenger mitoTEMPO during hyperoxia.  
49 Our finding that early life insults such as hyperoxia enhances the age-dependent expression of SARS-  
50 CoV-2 receptors in the respiratory epithelium helps explain why COVID-19 lung disease is greater in  
51 the elderly and people with pre-existing co-morbidities.

52  
53  
54

55 **Key Words:** Angiotensin Converting Enzyme 2, COVID-19, Hyperoxia, Mice, Transmembrane  
56 protease/serine subfamily member 2

57

## 58 INTRODUCTION

59 COVID-19 is an infectious disease of the lung caused by the severe acute respiratory  
60 syndrome coronavirus (SARS-CoV-2). As of July 2020, the World Health Organization reported this  
61 virus has infected more than 10 million people worldwide and killed approximately 500,000 people  
62 (<https://covid19.who.int>). Common symptoms include fever, cough, fatigue, shortness of breath, and  
63 loss of olfactory or gustatory function. While the majority of cases are mild, some people progress into  
64 severe acute respiratory distress syndrome, multi-organ failure, thrombosis, and septic shock. The  
65 severity of disease and mortality is highest among the elderly and people who have pre-existing lung  
66 or heart disease. There is growing evidence that asymptomatic children and young adults with  
67 COVID-19 may be at risk for heart disease, inflammatory vascular disease, and stroke <sup>1</sup>. People who  
68 were born preterm may be at great risk for COVID-19 because they are already at risk for  
69 hospitalization following infection with RSV, rhinovirus, human bocavirus, metapneumovirus, and  
70 parainfluenza viruses <sup>2</sup>. They may also develop pulmonary vascular disease and heart failure <sup>3,4</sup>,  
71 autism-like disorders <sup>5,6</sup>, and retinopathy <sup>7</sup> that puts them at further risk for COVID-19. Identifying  
72 mechanisms that drive susceptibility to pandemic viral infections like SARS-CoV-2 is therefore of  
73 great concern to susceptible individuals and their families.

74 The severity of COVID-19 is likely to be related to age-related changes in SARS-CoV-2  
75 receptors and how the immune system responds to infection <sup>1</sup>. Emerging evidence indicates high-risk  
76 individuals with SARS-CoV-2 have high rates of alveolar epithelial type 2 (AT2) cell infection,  
77 suggesting disease severity may be related to higher alveolar expression of the SARS-CoV-2 receptor  
78 angiotensin converting enzyme (ACE2) and its co-receptor transmembrane protease/serine subfamily  
79 member 2 (TMPRSS2) <sup>8,9</sup>. In fact, a recent meta-analysis of 700 people with predicted  
80 COVID-19 co-morbidities found that their lungs expressed high levels *Ace2* mRNA <sup>10</sup>. ACE2 is a zinc  
81 containing metalloprotease present at the surface of cells in the lung, heart, intestines, kidneys, and  
82 brain. It lowers blood pressure by catalyzing the hydrolysis of the vasoconstrictive molecule  
83 angiotensin II to angiotensin (1-7). ACE2 co-precipitates with transmembrane protease/serine  
84 subfamily member 2 (TMPRSS2) which hydrolyzes the S protein on coronaviruses, thus enabling viral

85 entry into infected cells<sup>9,11</sup>. Higher expression of these proteins in AT2 cells would theoretically lead  
86 to higher rates of infection in the distal lung. Infected AT2 cells produce inflammatory mediators that  
87 could contribute to a lethal cytokine storm<sup>12,13</sup>. They may also die. Loss of AT2 cells below a critical  
88 threshold could compromise alveolar homeostasis because they produce surfactant and serve as  
89 adult stem cells for the alveolar epithelium<sup>14</sup>. In fact, high rates of AT2 infection have been seen in  
90 people who have succumbed to H5N1, a highly pathogenic avian strain of influenza A virus<sup>15-17</sup>. But  
91 whether aging or pre-existing lung co-morbidities like preterm birth enhance the severity of respiratory  
92 viral infections via changing expression of viral receptors is not yet known.

93         Since preterm infants are exposed too soon to oxygen, we have been using mice to  
94 understand how high levels of oxygen at birth increases the severity of influenza A virus infection in  
95 adults. We previously reported how adult mice exposed to hyperoxia (100% oxygen) between  
96 postnatal days 0-4 develop persistent inflammation and fibrotic lung disease when infected with  
97 influenza A viruses HKx31 (H3N2) or PR8 (H1N1)<sup>18,19</sup>. Neonatal hyperoxia does not enhance primary  
98 infection<sup>20</sup> or clearance<sup>21</sup> of the virus. Instead, it reduced the number of adult AT2 cells by ~50%,  
99 thus lowering the number available to maintain alveolar homeostasis and epithelial regeneration after  
100 infection<sup>22</sup>. Because neonatal hyperoxia reduces the number of AT2 cells, we predicted it would  
101 reduce the alveolar expression of ACE2 and TMPRSS2 in the lung. Instead, we made the surprising  
102 discovery that expression of ACE2 and TMPRSS2 increases as mice age and this age-dependent  
103 expression can be enhanced by early exposure to hyperoxia. Our findings in mice suggest temporal  
104 and spatial changes in expression of SARS-CoV-2 receptors may contribute to the increased severity  
105 of COVID-19 seen in the elderly and people with pre-existing co-morbidities, including those born  
106 preterm.

107

## 108 RESULTS

109 *ACE2 is initially expressed by Club cells and then by AT2 cells as mice age.* The localization  
110 of ACE2 was examined in the lungs of mice between PND4 and 2 years of age by  
111 immunohistochemistry so as to better understand the temporal spatial pattern of its expression. ACE2  
112 was primarily detected in airway epithelial cells with minimal staining seen in the alveolar space  
113 (**Figure 1a**). The intensity of ACE2 staining increased steadily in the airway epithelium throughout the  
114 life of the mouse. A rare ACE2-positive alveolar cells (arrows) was first observed on PND7 and then  
115 steadily increased in number between 6 and 24 months of age. Western blotting for ACE2 confirmed  
116 that the abundance of ACE2 protein became progressively enriched in the whole lungs of 12- and 24-  
117 month-old mice relative to those of mice harvested at 2 months of age (**Figure 1b**). ACE2 mRNA  
118 levels were similarly increased in the whole lungs of 24-month-old mice than in those of mice  
119 harvested at 2 months of age (**Figure 1c**).

120 Co-staining with antibodies for ACE2 and the Club cell marker secretoglobin1a1 (Scgb1a1)  
121 showed extensive co-localization along the airways at both 2 and 12 months of age (**Figure 2a**), but  
122 the intensity of ACE2 staining was significantly higher at 12 months of age than at 2 months of age  
123 (**Figure 2b**). Co-staining for ACE2 and the AT2 cell marker proSP-C revealed that the vast majority of  
124 ACE2+ cells in the alveoli were AT2 cells (**Figure 2c**). Approximately 20% of proSP-C+ AT2 cells  
125 expressed ACE2 at 2 months while 80% of proSP-C+ AT2 cells expressed it at 12 months (**Figure**  
126 **2d**). These findings reveal that ACE2 is primarily expressed by the airway Club cells of young adult  
127 mice but becomes increasingly expressed by AT2 cells as mice age.

128  
129 *Neonatal hyperoxia enhances the age-dependent changes in ACE2 expression.* We  
130 previously showed that adult mice exposed to 100% oxygen between PND0-4 (**Figure 3a**) have fewer  
131 AT2 cells than mice exposed to room air<sup>23</sup> and thus expected ACE2 expression to be lower in the  
132 lungs of mice exposed to neonatal hyperoxia than in those of controls. It was therefore surprising to  
133 find that the levels of ACE2 protein were higher in the lungs of 2-month-old mice that were exposed to  
134 neonatal hyperoxia than in age-matched control lungs (**Figure 3b**). The levels of Ace2 mRNA were

135 also increased in the lungs of neonatal hyperoxia-exposed mice at 2 months of age and remained  
136 higher than in the lungs of age-matched controls at 6 and 12 months of age (**Figure 3c**). To determine  
137 the amount of oxygen needed to stimulate the expression of *Ace2*, the lungs of 2-month-old mice  
138 exposed to 0, 40, 60 or 80% oxygen from PND0-4 were examined by qRT-PCR (**Figure 3d**). While  
139 40% oxygen was not sufficient to induce *Ace2* mRNA, the levels of *Ace2* expression was significantly  
140 higher in mice exposed to 60% and 80% oxygen relative to controls. Exposing mice to a low chronic  
141 dose of oxygen (40% for 8 days) that does not alter alveolar development<sup>24</sup> also failed to increase  
142 *Ace2* levels relative to controls (data not shown). Because 40% oxygen for 8 days is higher  
143 cumulative dose of oxygen than 60% for 4 days, these findings suggest that oxygen alone may not be  
144 stimulating *Ace2* expression.

145 Immunohistochemistry was used to further understand how hyperoxia affected ACE2  
146 expression in the adult lung. While neonatal hyperoxia increased intensity of ACE2 staining in the  
147 airway, it most obviously increased the number of alveolar cells with detectable ACE2 (**Figure 4a**).  
148 When quantified, neonatal hyperoxia increased the number of alveolar cells expressing ACE2 by  
149 approximately 50% at 2, 6 and 12 months of age (**Figure 4b**). The increased alveolar expression  
150 seen at 2 months of age was primarily attributed to increased expression by proSP-C+ AT2 cells;  
151 however, this difference resolved at 6 and 12 months of age as more AT2 cells in control lungs began  
152 to express ACE2 (**Figure 4c**).

153  
154 *Anti-oxidants block oxygen-dependent changes in ACE2 expression.* Prior studies by us and other  
155 investigators showed that administering the mitochondrial superoxide scavenger mitoTEMPO to mice  
156 during exposure to hyperoxia (**Figure 5a**) prevents the alveolar simplification and cardiovascular  
157 disease observed when these mice reach adulthood<sup>25-27</sup>. qRT-PCR revealed administering  
158 mitoTEMPO during hyperoxia blunted the oxygen-dependent increase in *Ace2* mRNA seen in 2-  
159 month-old mice (**Figure 5a, b**). Immunohistochemistry confirmed mitoTEMPO reduced the number of  
160 AT2 cells with detectable levels of ACE2 protein (**Figure 5c, d**). It also reduced the intensity of ACE2  
161 staining in airway Club cells (**Figure 5e, f**). Interestingly, while mitoTEMPO did not affect ACE2

162 staining in control mice, it reduced the numbers of alveolar ACE2+ cells in the lungs of hyperoxia-  
163 exposed mice lower than controls.

164

165 *Neonatal hyperoxia stimulates age-dependent changes in TMPRSS2.* TMPRSS2 is an  
166 endoprotease expressed by respiratory epithelial cells that facilitates viral entry of coronaviruses into  
167 epithelial cells<sup>9</sup>. The levels of *Tmprss2* mRNA and protein were examined in the lungs of 2-, 12- and  
168 18-month-old mice that were exposed to neonatal hyperoxia and room air from PND0-4 by qRT-PCR  
169 and western blotting. *Tmprss2* mRNA was readily detected in the lungs of 2-month-old mice, and  
170 increased ~5-fold at 12 months and ~8-fold at 18 months (**Figure 6a**). Neonatal hyperoxia further  
171 increased *Tmprss2* expression by ~50% at each time-point examined. Western blotting similarly  
172 showed that the levels of TMPRSS2 protein were higher in the whole lung lysates of mice exposed to  
173 neonatal hyperoxia than in those of control mice (**Figure 6b**). As observed for *Ace2* expression,  
174 exposure to ≥ 60% oxygen from PND4-0 was required to significantly increase the levels of *Tmprss2*  
175 mRNA in the lungs of mice at 2 months of age (**Figure 6c**). Exposure to 40% oxygen from PND0-8  
176 also failed to change *Tmprss2* expression in adult mice (data not shown) while the administration of  
177 mitoTEMPO to mice during exposure blunted the effects of neonatal hyperoxia on *Tmprss2* mRNA  
178 (**Figure 6d**). Together, these findings suggest age and neonatal hyperoxia have similar effects on  
179 increasing TMPRSS2 as they do for ACE2.

180

181 **DISCUSSION**

182 The COVID-19 outbreak was first detected in the Chinese city of Wuhan in 2019 and has since  
183 expanded rapidly to become one of the worst pandemics to ever challenge the modern world. While  
184 people of all ages are susceptible to infection, the severity of disease is worse in people who are  
185 elderly or who have pre-existing health conditions including COPD, diabetes, hypertension, and  
186 cancer<sup>28</sup>. Those with multiple co-morbidities have a higher rate of mortality. People born preterm may  
187 also be at great risk for COVID-19 because they often suffer from multiple co-morbidities due, in part,  
188 to their lungs being exposed to oxygen too soon or to super-physiological concentrations used to  
189 maintain appropriate blood oxygen saturations. It is unclear whether co-morbidities increase disease  
190 by changing spatial and temporal expression of SARS-CoV-2 receptors or the immune response that  
191 leads to a lethal cytokine storm<sup>1</sup>. In this study, we present evidence that expression of the SARS-  
192 CoV-2 co-receptors ACE2 and TMPRSS2 increase in the respiratory epithelium of mice as they age  
193 and this can be stimulated or accelerated by early exposure to hyperoxia. Expression of ACE2 in  
194 distal AT2 cells was of particular interest because infection of these cells with other viruses has been  
195 associated with higher mortality in humans<sup>15-17</sup>. When infected such as by influenza A virus, AT2 cells  
196 may contribute to lung disease by producing inflammatory molecules that contribute to a lethal  
197 cytokine storm<sup>12</sup>. They may also die and therefore reduce the number of surviving AT2 cells required  
198 to serve as stem cells for alveolar regeneration<sup>22,29,30</sup>. Our findings support the idea that age and co-  
199 morbidities like preterm birth may increase the severity of COVID-19 by changing temporal and spatial  
200 patterns of SARS-CoV-2 receptors.

201 We found that ACE2 was primarily expressed by airway Club cells during early postnatal life.  
202 The intensity of ACE2 staining increased in the airways of mice with age and became detectable in  
203 the alveoli of young adult mice. Co-localization with proSP-C revealed that most, but not all alveolar  
204 cells expressing ACE2 were AT2 cells. Our findings are consistent with an earlier study showing that  
205 ACE2 is expressed in the adult mouse lung by Clara cells (now called Club cells), AT2 cells, and to  
206 some extent by endothelial cells around small and medium sized vessels<sup>31</sup>. While that study showed  
207 how ACE2 levels rise during fetal development, our findings extend it by showing that ACE2

208 expression continues to increase as mice age. We also found that *Tmprss2* mRNA expression  
209 increases as mice age and this expression was similarly enhanced by neonatal hyperoxia. While AT2  
210 cells have previously been shown to express TMPRSS2<sup>11</sup>, we were not able to detect it in the mouse  
211 lung using commercially available antibodies. However, we did find that the abundance of *Tmprss2*  
212 mRNA and protein abundance increased with age and neonatal hyperoxia, and was reduced by  
213 mitoTEMPO similar to that of *Ace2*. The higher expression of these genes as mice age is in  
214 agreement with recent review that discussed two unpublished studies deposited in *bioRxiv* showing  
215 how expression of *Ace2* and *Tmprss2* mRNA increases with age in human respiratory epithelium<sup>1</sup>.  
216 Those findings in humans and ours in mice suggest the age-dependent increase in SARS2-CoV-2  
217 receptors may be responsible for increasing the severity of COVID-19 lung disease in elderly people.

218 It is important to recognize the normal functions of ACE2 and TMPRSS2 because that may  
219 help explain why their expression steadily increases with age<sup>32</sup>. ACE2 is perhaps best known for its  
220 role in controlling blood pressure in the renin-angiotensin system<sup>33</sup>. ACE1 converts the 10-amino acid  
221 angiotensin I to an 8-amino acid vasoconstrictive peptide called angiotensin II. ACE2 accumulates in  
222 people with pulmonary hypertension and hydrolyzes Angiotensin II to Ang(1-7), which has  
223 vasodilation properties. Over-expressing ACE2 also protects against right ventricular hypertrophy<sup>34</sup>.  
224 Hence, higher levels of ACE2 seen as the lung ages may reflect an adaptive response designed to  
225 protect against the development of cardiovascular disease. Interestingly, ACE2 levels decline in  
226 bleomycin-induced lung fibrosis and humans with interstitial pulmonary fibrosis while angiotensin II  
227 levels rise<sup>35,36</sup>. Angiotensin II can promote fibrosis by stimulating AT2 cell apoptosis downstream of  
228 TGF- $\beta$  signaling<sup>37</sup>. ACE2 serves as an anti-fibrotic molecule by stimulating the hydrolysis of  
229 angiotensin II to Ang(1-7), which in turn signals through the Mas oncogene to block AT2 cell apoptosis  
230 by suppressing JNK activation<sup>38</sup>. The slow and steady increase in ACE2 expression as the lung ages  
231 may also serve to preserve AT2 cells and thus reduce or prevent the development of idiopathic  
232 pulmonary fibrosis. In contrast to ACE2, the normal role of TMPRSS2 in the lung is poorly understood.  
233 TMPRSS2 is a serine protease that is localized to the apical surface of secretory cells such as Club  
234 and AT2 cells of the lung<sup>39</sup>. Its expression is highly regulated by androgens in the prostate gland and

235 may be similarly responsive to androgens in the lung, suggesting it may play a role in sex-dependent  
236 differences in the lung.

237 Our study also found that neonatal hyperoxia increased or accelerated expression of *Ace2*  
238 mRNA, ACE2 protein, and *Tmprss2* mRNA as mice age. Significant changes were seen with 60% or  
239 more FiO<sub>2</sub> at 8 weeks (2 months) of age and persisted as mice age. How hyperoxia regulates  
240 expression of these proteins is conflicting and remains to be better understood. One study using  
241 human fetal IMR-90 fibroblasts found that hyperoxia does not change expression of ACE2<sup>40</sup>.  
242 However, ACE2 was depleted when cells returned to room air presumably because it was being  
243 proteolyzed and shed into the media. In contrast, another study found higher levels of ACE2 in  
244 newborn rats exposed to 95% oxygen for the first week of life and then recovered in 60% oxygen for  
245 the next two weeks<sup>41</sup>. In our hands, changes in *Ace2* or *Tmprss2* mRNA were first detected in 8-  
246 week-old mice exposed to hyperoxia between PND0-4. We did not detect changes at the end of  
247 oxygen exposure (PND4). In fact, we recently deposited an RNA-seq analysis of AT2 cells isolated  
248 from PND4 mice exposed to room air versus hyperoxia that shows hyperoxia modestly inhibits *Ace2*  
249 and increases *Tmprss2* mRNA abundance (Gene Expression Omnibus of the National Center for  
250 Biotechnology Information under the accession number GSE140915). This suggests neonatal  
251 hyperoxia may not affect expression until after the mice are returned to room air. Because ACE2 and  
252 TMPRSS2 were only affected by doses of oxygen that cause long-term changes in lung function (i.e.,  
253 60% for 4 days but not 40% for 4 or 8 days), we speculate that they occur as an adaptive response to  
254 the alveolar simplification and cardiovascular disease as mice exposed to neonatal oxygen age. The  
255 elevated expression of ACE2 and perhaps TMPRSS2 may serve to prevent the loss of AT2 cells  
256 damaged by early oxygen and promote vasodilation as the pulmonary capillary bed undergoes  
257 rarefaction<sup>23,42</sup>. But higher levels of these proteins may become a maladaptive response when they  
258 render the lung more susceptible to coronavirus infections.

259 While it remains to be determined how age or oxygen regulate expression of ACE2 and  
260 TMPRSS2, our studies with mitoTEMPO suggest their expression may be influenced by oxidative  
261 stress. Administering mitoTEMPO, a scavenger of mitochondrial superoxide during hyperoxia blunted

262 the oxygen-dependent increase in these genes detected in 2-month-old mice. Because hyperoxia  
263 progressively increases mitochondrial oxidation, it has historically been used to model aging-related  
264 oxidative stress<sup>43</sup>. This implies mitochondrial oxidation that accumulates as the lung ages steadily  
265 increases expression of ACE2 and TMPRSS2, which in turn may then attempt to defend against the  
266 pathological changes attributed to the aging process. Anti-oxidant therapies may therefore prove  
267 useful for suppressing expression of SARS-CoV-2 receptors and reducing the severity of COVID-19  
268 related lung disease, especially in people with pre-existing co-morbidities.

269 Increased expression of ACE2 and TMPRSS2 may not be the only way these proteins  
270 enhance the severity of COVID-19-related lung disease. For example, TMPRSS2 facilitates viral  
271 activation and entry by cleaving hemagglutinin on influenza A virus and the spike protein on the  
272 SARS-CoV-2 virus<sup>11</sup>. The spike protein accesses the cell when it binds the glucose regulated protein  
273 78 (Grp78, BiP) found on the cell surface<sup>44</sup>. Grp78 is a master regulator of the unfolded protein  
274 response (UPR)<sup>45</sup>. It is normally localized to the endoplasmic reticulum (ER) where it inhibits the UPR  
275 by binding Activating Transcription Factor 6 (ATF6), Protein kinase RNA-like Endoplasmic Reticulum  
276 Kinase (PERK), and Inositol-requiring Enzyme 1 (IRE1). Grp78 is released from these proteins when  
277 oxidation and other stressful conditions cause an accumulation of unfolded proteins. It can then  
278 escape the ER and traffic to the cell surface where it becomes available to bind the coronavirus S  
279 protein and facilitate viral entry. This information should raise great concern for people with familial  
280 forms of IPF caused by mutations in *SFTPC* and other genes that activate the UPR in AT2 cells<sup>46</sup>.  
281 Genetic studies in mice suggest mutant forms of SP-C that activate the UPR are not sufficient by  
282 themselves to cause fibrotic lung disease. However, they can predispose the lung to fibrotic disease  
283 following viral infections<sup>47</sup>. Familial forms of IPF that activate the UPR in AT2 cells may therefore  
284 accelerate the age-dependent susceptibility of AT2 cells to SARS-CoV-2 infections.

285 In summary, we found that neonatal hyperoxia increases or accelerates the age-dependent  
286 expression of ACE2 and TMPRSS2 in the airway and alveolar epithelium of mice. Understanding how  
287 expression of these proteins changes with age and in response to early life insults such as neonatal

288 hyperoxia may provide new opportunities for reducing the severity of COVID-19 and other types of  
289 lung disease.

## 290 MATERIALS AND METHODS

291 *Mice.* C57BL/6J mice were purchased from the Jackson Laboratories and maintained as an  
292 inbred colony. Mice were exposed to room air (21% oxygen) as control or hyperoxia (100% oxygen  
293 unless otherwise stated) between birth and postnatal day (PND) 4 and then returned to room air<sup>19</sup>.  
294 Dams were cycled every 24 hours to ensure that hyperoxia did not compromise their health. Some  
295 mice exposed to room air or hyperoxia were injected intraperitoneally with 0.7µg/g mitoTEMPO (Enzo  
296 Life Sciences, Farmingdale, NY) or vehicle (phosphate-buffered saline) on PND0, PND1, and PND2.  
297 All mice used in this study were of mixed sex and housed in a pathogen-free environment according  
298 to a protocol (UCAR2007-121E) approved by the University Committee on Animal Resources at the  
299 University of Rochester.

300  
301 *Immunohistochemistry.* Lungs were inflation fixed overnight in 10% neutral buffered formalin,  
302 embedded in paraffin and 4 µm sections prepared<sup>23,48</sup>. Sections were stained with antibodies against  
303 ACE2 (Invitrogen, PA5-47488, Waltham, MA), Scgb1a1 (Sigma, 07-063, St. Louis, MO) and proSP-C  
304 (Seven Hills Bioreagents, Cincinnati, OH). Immune complexes were detected with fluorescently  
305 labeled secondary antibody (Jackson Immune Research, West Grove, PA). Sections were then  
306 stained with 4', 6-diamidino-2-phenylindole (DAPI) (Life Technologies, Carlsbad, CA) before viewing  
307 with Nikon E800 Fluorescence microscope (Microvideo Instruments, Avon, MA) and a SPOT-RT  
308 digital camera (Diagnostic Instruments, Sterling Heights, MI).

309  
310 *Quantitative RT-PCR.* Total RNA was isolated from the lung using Trizol reagent  
311 (ThermoFisher Scientific) and reverse transcribed to cDNA using the iScript cDNA synthesis kit (Bio-  
312 Rad Laboratories, Hercules, CA). The cDNA was then amplified with SYBR Green I dye on CFX96™  
313 or CFX384™ Real-Time PCR detection system (Bio-Rad Laboratories, Hercules, CA). PCR products  
314 were amplified with sequence-specific primers for mouse *Ace2* (sense 5'-  
315 GGATACCTACCCTTCCTACATCAGC-3' and antisense CTACCCACATATCACCAAGCA-3'),  
316 *Tmprss2* (sense 5'- TACTTGGAGCGGACGAGGAA-3', and antisense 5'-

317 AGGAGGTCAGTATGGGGCTT-3') or 18S rRNA (sense 5-CGGCTACCATCCAAGGAA-3', and  
318 antisense 5'- GCTGGAATTACCGCGGCT- 3') used to normalize equal loading of the template  
319 cDNAs. Amplifications were conducted with iTaq Universal SYBR Green Master Mix (Bio-Rad  
320 Laboratories, Hercules, CA). Fold changes in gene expression were calculated by the  $\Delta\Delta C_t$  method  
321 using the  $C_t$  values for the housekeeping 18S rRNA as a control for loading.

322

323 *Western blot analysis.* The left lung lobe was homogenized in lysis buffer and insoluble  
324 material removed by centrifugation<sup>23</sup>. Equal amounts of protein were separated on sodium dodecyl  
325 sulfate polyacrylamide gels and transferred to nylon membranes. The membranes were  
326 immunoblotted with primary antibodies to ACE2 (Invitrogen, PA5-47488, Waltham, MA), TMPRSS2  
327 (Abcam, ab92323, Cambridge, MA) or  $\beta$ -ACTIN (Sigma, A2066). The blots were then incubated in  
328 appropriate secondary antibody (Southern Biotech, Birmingham, AL). Immune complexes were  
329 detected by chemiluminescence and visualized with a ChemiDoc Imaging System (Bio-Rad  
330 Laboratories, Hercules, CA).

331

332 *Statistical Analysis.* Data were evaluated using JMP14 software (SAS Institute, Cary, NC) and  
333 graphed as means  $\pm$  SEM. An unpaired t-test and 2-way ANOVA were used to determine overall  
334 significance, followed by Tukey-Kramer HSD tests.

335

336 REFERENCES

- 337 1 Lingappan, K., Karmouty-Quintana, H., Davies, J., Akkanti, B. & Harting, M. T. Understanding  
338 the age divide in COVID-19: why are children overwhelmingly spared? *Am J Physiol Lung Cell*  
339 *Mol Physiol* **319**, L39-L44, doi:10.1152/ajplung.00183.2020 (2020).
- 340 2 Garcia-Garcia, M. L. *et al.* Clinical and Virological Characteristics of Early and Moderate  
341 Preterm Infants Readmitted With Viral Respiratory Infections. *The Pediatric infectious disease*  
342 *journal* **34**, 693-699, doi:10.1097/INF.0000000000000718 (2015).
- 343 3 Eber, E. & Zach, M. S. Long term sequelae of bronchopulmonary dysplasia (chronic lung  
344 disease of infancy). *Thorax* **56**, 317-323, doi:10.1136/thorax.56.4.317 (2001).
- 345 4 Bensley, J. G., De Matteo, R., Harding, R. & Black, M. J. The effects of preterm birth and its  
346 antecedents on the cardiovascular system. *Acta obstetricia et gynecologica Scandinavica* **95**,  
347 652-663, doi:10.1111/aogs.12880 (2016).
- 348 5 Doyle, L. W. & Anderson, P. J. Pulmonary and neurological follow-up of extremely preterm  
349 infants. *Neonatology* **97**, 388-394, doi:10.1159/000297771 (2010).
- 350 6 Vaucher, Y. E. *et al.* Neurodevelopmental outcomes in the early CPAP and pulse oximetry  
351 trial. *N Engl J Med* **367**, 2495-2504, doi:10.1056/NEJMoa1208506 (2012).
- 352 7 Stenson, B. J. *et al.* Oxygen saturation and outcomes in preterm infants. *N Engl J Med* **368**,  
353 2094-2104, doi:10.1056/NEJMoa1302298 (2013).
- 354 8 McCray, P. B., Jr. *et al.* Lethal infection of K18-hACE2 mice infected with severe acute  
355 respiratory syndrome coronavirus. *J Virol* **81**, 813-821, doi:10.1128/JVI.02012-06 (2007).
- 356 9 Shulla, A. *et al.* A transmembrane serine protease is linked to the severe acute respiratory  
357 syndrome coronavirus receptor and activates virus entry. *J Virol* **85**, 873-882,  
358 doi:10.1128/JVI.02062-10 (2011).
- 359 10 Pinto, B. G. G. *et al.* ACE2 Expression is Increased in the Lungs of Patients with Comorbidities  
360 Associated with Severe COVID-19. *J Infect Dis*, doi:10.1093/infdis/jiaa332 (2020).
- 361 11 Glowacka, I. *et al.* Evidence that TMPRSS2 activates the severe acute respiratory syndrome  
362 coronavirus spike protein for membrane fusion and reduces viral control by the humoral  
363 immune response. *J Virol* **85**, 4122-4134, doi:10.1128/JVI.02232-10 (2011).
- 364 12 Wang, J. *et al.* Innate immune response to influenza A virus in differentiated human alveolar  
365 type II cells. *Am J Respir Cell Mol Biol* **45**, 582-591, doi:10.1165/rcmb.2010-0108OC (2011).
- 366 13 McCormack, F. X. & Whitsett, J. A. The pulmonary collectins, SP-A and SP-D, orchestrate  
367 innate immunity in the lung. *J Clin Invest* **109**, 707-712, doi:10.1172/JCI15293 (2002).
- 368 14 Barkauskas, C. E. *et al.* Type 2 alveolar cells are stem cells in adult lung. *J Clin Invest* **123**,  
369 3025-3036, doi:10.1172/JCI68782 (2013).
- 370 15 Yao, L., Korteweg, C., Hsueh, W. & Gu, J. Avian influenza receptor expression in H5N1-  
371 infected and noninfected human tissues. *Faseb J* **22**, 733 - 740 (2008).
- 372 16 Gu, J. *et al.* H5N1 infection of the respiratory tract and beyond: a molecular pathology study.  
373 *Lancet* **370**, 1137-1145 (2007).
- 374 17 van Riel, D. *et al.* H5N1 Virus Attachment to Lower Respiratory Tract. *Science* **312**, 399,  
375 doi:10.1126/science.1125548 (2006).
- 376 18 O'Reilly, M. A., Marr, S. H., Yee, M., McGrath-Morrow, S. A. & Lawrence, B. P. Neonatal  
377 hyperoxia enhances the inflammatory response in adult mice infected with influenza A virus.  
378 *American Journal of Respiratory and Critical Care Medicine* **177**, 1103-1110,  
379 doi:10.1164/rccm.200712-1839OC (2008).
- 380 19 Buczynski, B. W., Yee, M., Martin, K. C., Lawrence, B. P. & O'Reilly, M. A. Neonatal hyperoxia  
381 alters the host response to influenza A virus infection in adult mice through multiple pathways.  
382 *Am J Physiol Lung Cell Mol Physiol* **305**, L282-290, doi:10.1152/ajplung.00112.2013 (2013).
- 383 20 Domm, W. *et al.* Oxygen-dependent changes in lung development do not affect epithelial  
384 infection with influenza A virus. *Am J Physiol Lung Cell Mol Physiol* **313**, L940-L949,  
385 doi:10.1152/ajplung.00203.2017 (2017).
- 386 21 Giannandrea, M., Yee, M., O'Reilly, M. A. & Lawrence, B. P. Memory CD8+ T cells are  
387 sufficient to alleviate impaired host resistance to influenza A virus infection caused by neonatal

- 388 oxygen supplementation. *Clinical and vaccine immunology : CVI* **19**, 1432-1441,  
389 doi:10.1128/CVI.00265-12 (2012).
- 390 22 Yee, M. *et al.* Alternative Progenitor Lineages Regenerate the Adult Lung Depleted of Alveolar  
391 Epithelial Type 2 Cells. *Am J Respir Cell Mol Biol* **56**, 453-464, doi:10.1165/rcmb.2016-  
392 0150OC (2017).
- 393 23 Yee, M. *et al.* Type II epithelial cells are critical target for hyperoxia-mediated impairment of  
394 postnatal lung development. *Am J Physiol Lung Cell Mol Physiol* **291**, L1101-1111,  
395 doi:10.1152/ajplung.00126.2006 (2006).
- 396 24 Dylag, A. M., Haak, J., Yee, M. & O'Reilly, M. A. Pulmonary mechanics and structural lung  
397 development after neonatal hyperoxia in mice. *Pediatric research* **87**, 1201-1210,  
398 doi:10.1038/s41390-019-0723-y (2020).
- 399 25 Yee, M. *et al.* Neonatal hyperoxia depletes pulmonary vein cardiomyocytes in adult mice via  
400 mitochondrial oxidation. *Am J Physiol Lung Cell Mol Physiol* **314**, L846-L859,  
401 doi:10.1152/ajplung.00409.2017 (2018).
- 402 26 Datta, A. *et al.* Mouse lung development and NOX1 induction during hyperoxia are  
403 developmentally regulated and mitochondrial ROS dependent. *Am J Physiol Lung Cell Mol*  
404 *Physiol* **309**, L369-377, doi:10.1152/ajplung.00176.2014 (2015).
- 405 27 Farrow, K. N. *et al.* Brief hyperoxia increases mitochondrial oxidation and increases  
406 phosphodiesterase 5 activity in fetal pulmonary artery smooth muscle cells. *Antioxidants &*  
407 *redox signaling* **17**, 460-470, doi:10.1089/ars.2011.4184 (2012).
- 408 28 Guan, W. J. *et al.* Comorbidity and its impact on 1590 patients with COVID-19 in China: a  
409 nationwide analysis. *The European respiratory journal : official journal of the European Society*  
410 *for Clinical Respiratory Physiology* **55**, doi:10.1183/13993003.00547-2020 (2020).
- 411 29 Garcia, O. *et al.* Targeted Type 2 Alveolar Cell Depletion. A Dynamic Functional Model for  
412 Lung Injury Repair. *Am J Respir Cell Mol Biol* **54**, 319-330, doi:10.1165/rcmb.2014-0246OC  
413 (2016).
- 414 30 Sisson, T. H. *et al.* Targeted injury of type II alveolar epithelial cells induces pulmonary  
415 fibrosis. *Am J Respir Crit Care Med* **181**, 254-263, doi:10.1164/rccm.200810-1615OC (2010).
- 416 31 Wiener, R. S., Cao, Y. X., Hinds, A., Ramirez, M. I. & Williams, M. C. Angiotensin converting  
417 enzyme 2 is primarily epithelial and is developmentally regulated in the mouse lung. *Journal of*  
418 *cellular biochemistry* **101**, 1278-1291, doi:10.1002/jcb.21248 (2007).
- 419 32 Samavati, L. & Uhal, B. D. ACE2, Much More Than Just a Receptor for SARS-COV-2. *Front*  
420 *Cell Infect Microbiol* **10**, 317, doi:10.3389/fcimb.2020.00317 (2020).
- 421 33 Gheblawi, M. *et al.* Angiotensin-Converting Enzyme 2: SARS-CoV-2 Receptor and Regulator  
422 of the Renin-Angiotensin System: Celebrating the 20th Anniversary of the Discovery of ACE2.  
423 *Circulation research* **126**, 1456-1474, doi:10.1161/CIRCRESAHA.120.317015 (2020).
- 424 34 Ferreira, A. J. *et al.* Evidence for angiotensin-converting enzyme 2 as a therapeutic target for  
425 the prevention of pulmonary hypertension. *Am J Respir Crit Care Med* **179**, 1048-1054,  
426 doi:10.1164/rccm.200811-1678OC (2009).
- 427 35 Li, X. *et al.* Angiotensin converting enzyme-2 is protective but downregulated in human and  
428 experimental lung fibrosis. *Am J Physiol Lung Cell Mol Physiol* **295**, L178-185,  
429 doi:10.1152/ajplung.00009.2008 (2008).
- 430 36 Marshall, R. P. *et al.* Angiotensin II and the fibroproliferative response to acute lung injury. *Am*  
431 *J Physiol Lung Cell Mol Physiol* **286**, L156-164, doi:10.1152/ajplung.00313.2002 (2004).
- 432 37 Papp, M., Li, X., Zhuang, J., Wang, R. & Uhal, B. D. Angiotensin receptor subtype AT(1)  
433 mediates alveolar epithelial cell apoptosis in response to ANG II. *Am J Physiol Lung Cell Mol*  
434 *Physiol* **282**, L713-718, doi:10.1152/ajplung.00103.2001 (2002).
- 435 38 Uhal, B. D., Li, X., Xue, A., Gao, X. & Abdul-Hafez, A. Regulation of alveolar epithelial cell  
436 survival by the ACE-2/angiotensin 1-7/Mas axis. *Am J Physiol Lung Cell Mol Physiol* **301**,  
437 L269-274, doi:10.1152/ajplung.00222.2010 (2011).
- 438 39 Stopsack, K. H., Mucci, L. A., Antonarakis, E. S., Nelson, P. S. & Kantoff, P. W. TMPRSS2  
439 and COVID-19: Serendipity or Opportunity for Intervention? *Cancer Discov* **10**, 779-782,  
440 doi:10.1158/2159-8290.CD-20-0451 (2020).

- 441 40 Oarhe, C. I. *et al.* Hyperoxia downregulates angiotensin-converting enzyme-2 in human fetal  
442 lung fibroblasts. *Pediatric research* **77**, 656-662, doi:10.1038/pr.2015.27 (2015).
- 443 41 Jiang, J. S. *et al.* Activation of the renin-angiotensin system in hyperoxia-induced lung fibrosis  
444 in neonatal rats. *Neonatology* **101**, 47-54, doi:10.1159/000329451 (2012).
- 445 42 Yee, M. *et al.* Neonatal hyperoxia causes pulmonary vascular disease and shortens life span  
446 in aging mice. *Am J Pathol* **178**, 2601-2610, doi:10.1016/j.ajpath.2011.02.010 (2011).
- 447 43 Joenje, H. Genetic toxicology of oxygen. *Mutation research* **219**, 193-208, doi:10.1016/0921-  
448 8734(89)90001-5 (1989).
- 449 44 Ibrahim, I. M., Abdelmalek, D. H., Elshahat, M. E. & Elfiky, A. A. COVID-19 spike-host cell  
450 receptor GRP78 binding site prediction. *J Infect* **80**, 554-562, doi:10.1016/j.jinf.2020.02.026  
451 (2020).
- 452 45 Ron, D. & Walter, P. Signal integration in the endoplasmic reticulum unfolded protein  
453 response. *Nat Rev Mol Cell Biol* **8**, 519-529 (2007).
- 454 46 Zoz, D. F., Lawson, W. E. & Blackwell, T. S. Idiopathic pulmonary fibrosis: a disorder of  
455 epithelial cell dysfunction. *The American journal of the medical sciences* **341**, 435-438,  
456 doi:10.1097/MAJ.0b013e31821a9d8e (2011).
- 457 47 Bridges, J. P., Xu, Y., Na, C. L., Wong, H. R. & Weaver, T. E. Adaptation and increased  
458 susceptibility to infection associated with constitutive expression of misfolded SP-C. *J Cell Biol*  
459 **172**, 395-407, doi:10.1083/jcb.200508016 (2006).
- 460 48 Yee, M. *et al.* Neonatal oxygen adversely affects lung function in adult mice without altering  
461 surfactant composition or activity. *Am J Physiol Lung Cell Mol Physiol* **297**, L641-649,  
462 doi:10.1152/ajplung.00023.2009 (2009).
- 463

464 **ACKNOWLEDGEMENTS**

465 We thank Robert Gelein for maintaining the oxygen exposure facility and Daria Krenitsky for  
466 tissue processing and sectioning. This work was funded, in part, by National Institutes of Health  
467 Grants R01 HL091968 (M. A. O'Reilly), NIH Center Grant P30 ES001247, and a generous startup  
468 package from the Department of Pediatrics (A. M. Dylag). The University of Rochester's Department  
469 of Pediatrics provided financial support through the Perinatal and Pediatric Origins of Disease  
470 Program.

471

472 **AUTHOR CONTRIBUTIONS**

473 M.Y. designed and conducted experiments, analyzed the data, prepared figures, and helped  
474 write the manuscript; E.C. performed experiments and helped write the manuscript; J.H., performed  
475 experiments; A.D. aided in experimental design; M.O. designed the experimental research, analyzed  
476 the data, and wrote the manuscript. All authors reviewed and approved the final version of the  
477 manuscript.

478

479 **COMPETING INTEREST STATEMENT**

480 The author(s) declare no competing interests.

481 **FIGURE LEGENDS**

482

483 **Figure 1.** ACE2 expression changes in lung as mice age. **(a)** Lungs harvested from mice of different  
484 ages were stained for ACE2 (red) and counterstained with DAPI (blue). ACE2 was detected in  
485 airways of all mice and alveolar regions (yellow arrows). Bar = 100  $\mu$ m. **(b)** Lungs homogenates  
486 prepared from 2-month, 12-month, and 24-month-old mice were immunoblotted for ACE2 and  $\beta$ -  
487 ACTIN as a loading control. Each lane represents an individual mouse. Band intensity of ACE2 to  $\beta$ -  
488 ACTIN was quantified and graphed as fold change relative to 2-month samples. Bars reflect mean  $\pm$   
489 SD graphed. **(c)** qRT-PCR was used to quantify *Ace2* mRNA in total lung homogenates of 2-month  
490 and 24-month-old mice. Data is graphed as the fold change of *Ace2* after normalizing to *18S* RNA.  
491 Bars reflect mean  $\pm$  SD graphed as fold change over 2-month values. Statistical significance is  
492 comparisons for all pairs using Tukey-Kramer HSD test, with \* $P \leq 0.05$ ; \*\* $P \leq 0.01$ .

493

494 **Figure 2.** Aging increases ACE2 expression in airway Club and alveolar type 2 cells. **(a)** Lungs from  
495 2-month and 12-month-old mice were immunostained for ACE2 (red), *Scgb1a1* (green), and  
496 counterstained with DAPI (blue). Boxed sections are individual ACE2 and *Scgb1a1* stains. **(b)**  
497 Quantitation of ACE2 Red staining intensity. All the cells were imaged using identical exposure time.  
498 Scale bar = 50  $\mu$ m. **(c)** Lungs were stained for ACE2 (red), proSP-C (green), and counterstained with  
499 DAPI (blue). Boxed sections are enlarged below each figure. **(d)** The proportion of proSP-C+ cells  
500 expressing ACE2 was quantified and graphed. Statistical significance is comparisons for all pairs  
501 using Tukey-Kramer HSD test, with \*\* $P \leq 0.01$ ; \*\*\* $P \leq 0.001$ . Bar = 50  $\mu$ m.

502

503 **Figure 3.** Neonatal hyperoxia stimulates expression of ACE2 in adult mice. **(a)** Cartoon showing the  
504 experimental approach of exposing newborn mice to hyperoxia. **(b)** Total lung homogenates were  
505 immunoblotted for ACE2 and  $\beta$ -ACTIN as a loading control. Data is graphed as mean  $\pm$  SD fold  
506 change over room air values. **(c)** qRT-PCR was used to quantify *Ace2* mRNA in total lung

507 homogenates of 2-, 12-, and 18-month-old mice exposed to room air or hyperoxia between PND0-4.  
508 Values were normalized to expression of 18S RNA and graphed as mean  $\pm$  SD fold change of ACE2  
509 in 2-month-old room air mice. (d) qRT-PCR was used to quantify *Ace2* mRNA in total lung  
510 homogenates of 2-month-old mice exposed to room air, 40%, 60%, or 80% oxygen between PND0-4.  
511 Values were normalized to expression of 18S RNA and graphed as fold change of ACE2 in 2 month  
512 room air mice. Statistical significance is comparisons for all pairs using Tukey-Kramer HSD test with  
513 \*P $\leq$ 0.05; \*\*P $\leq$ 0.01; \*\*\*P $\leq$ 0.001.

514

515 **Figure 4.** Neonatal hyperoxia stimulates expression of ACE2 in alveolar type 2 cells. (a) Lungs of 2-,  
516 6- and 12-month-old mice exposed to room air or hyperoxia between pnd0-4 were stained for ACE2  
517 (red), proSP-C (green), and DAPI. Upper rows reflect room air and lower rows reflect hyperoxia  
518 between PND0-4. Boxed regions are enlarged to the right of each image. (b) The proportion of ACE2-  
519 positive to total DAPI cells was quantified and graphed. (c) The proportion of proSP-C+ cells that  
520 express ACE2 were quantified and graphed. Values in b, c represent mean  $\pm$  SD of 4-5 lungs per  
521 group with stated P values in the graphs. Statistical significance is comparisons for all pairs using  
522 Tukey-Kramer HSD test with \*P $\leq$ 0.05.

523

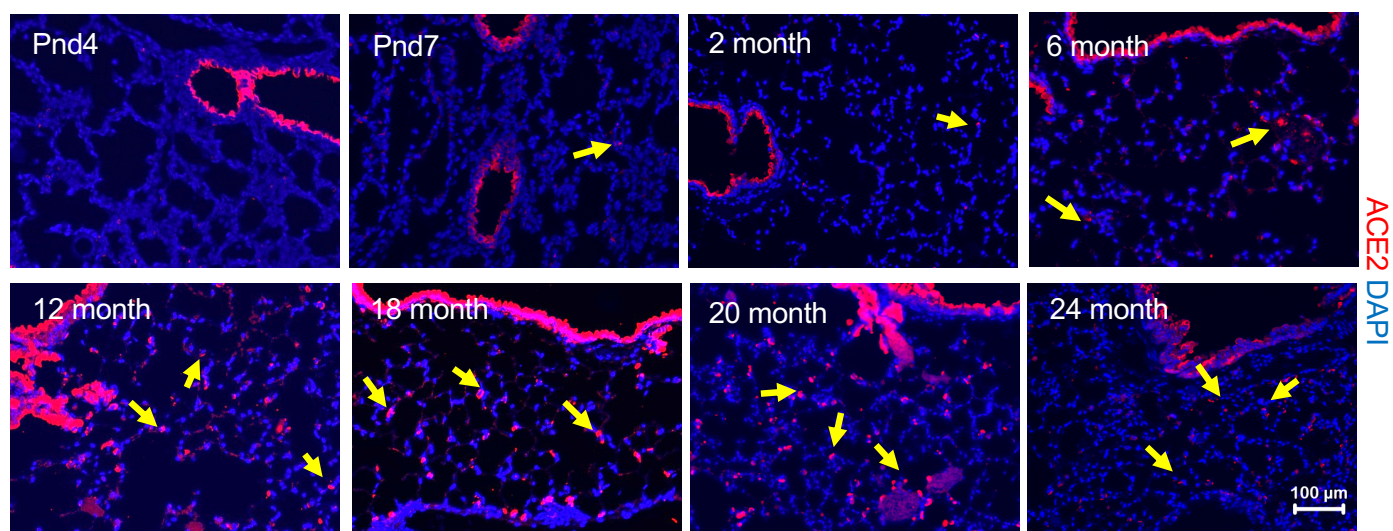
524 **Figure 5.** Anti-oxidants prevent hyperoxia from stimulating expression of ACE2. (a) Cartoon showing  
525 the experimental approach of exposing newborn mice to hyperoxia and treated with mitoTEMPO (d1-  
526 d3). (b) qRT-PCR was used to measure *Ace2* mRNA expression in 2-month-old mice exposed to  
527 room air or hyperoxia as vehicle or mitoTEMPO between PND0-4. Values reflect mean  $\pm$  SD of 4-5  
528 mice per group and graphed as fold change over mice administered room air and vehicle control.  
529 Expression of *Ace2* mRNA was normalized to 18S rRNA and mean  $\pm$  SD values graphed relative to  
530 room air values. (c) Lung alveoli were stained for ACE2 (red), and counterstained with DAPI (blue).  
531 (d) Total % of ACE2 cells in lung alveoli. (e) Lung-airways were stained for ACE2 (red), and  
532 counterstained with DAPI (blue). (f) Quantitation of ACE2 Red staining intensity. All the cells were  
533 imaged using identical exposure time. Scale bar = 50  $\mu$ m; Quantitation of ACE2 Red was derived from

534 images. Statistical significance is comparisons for all pairs using Tukey-Kramer HSD test with  
535 \* $P \leq 0.05$ ; \*\* $P \leq 0.01$ ; \*\*\* $P \leq 0.001$ .

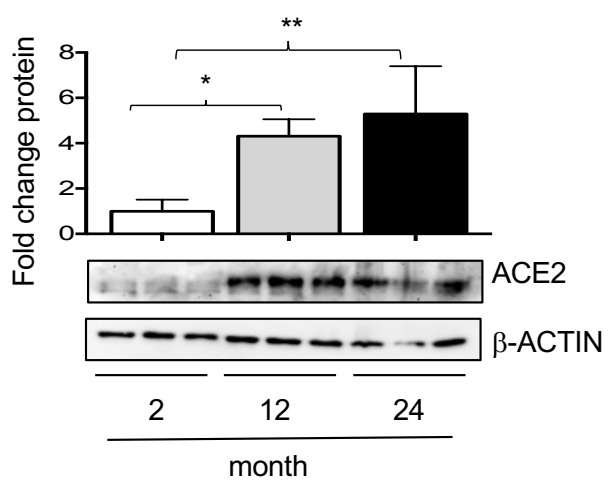
536

537 **Figure 6.** Neonatal hyperoxia stimulates age-dependent expression of *Tmprss2* mRNA. **(a)** qRT-PCR  
538 was used to quantify *Tmprss2* mRNA in total lung homogenates of 2-, 12-, and 18-month-old mice  
539 exposed to room air or hyperoxia between PND0-4. Values were normalized to expression of *18S*  
540 RNA and graphed as fold change of ACE2 in 2-month-old room air mice. **(b)** Western blot-based  
541 quantification of TMPRSS2. Data in panels A-D reflect mean  $\pm$  SD and graphed as fold change  
542 relative to control mice exposed to room air. **(c)** qRT-PCR was used to measure *Tmprss2* mRNA in  
543 total lung homogenates of 2 month mice exposed to room air, 40%, 60%, or 80% oxygen between  
544 PND0-4. **(d)** qRT-PCR was used to measure *Tmprss2* mRNA in control and 2-month-old mice  
545 exposed to room air or hyperoxia and vehicle or mitoTEMPO between PND0-4 N=4-5 mice per group.  
546 Statistical significance is comparisons for all pairs using Tukey-Kramer HSD test with \* $P \leq 0.05$ ;  
547 \*\* $P \leq 0.01$ .

**a**



**b**



**c**

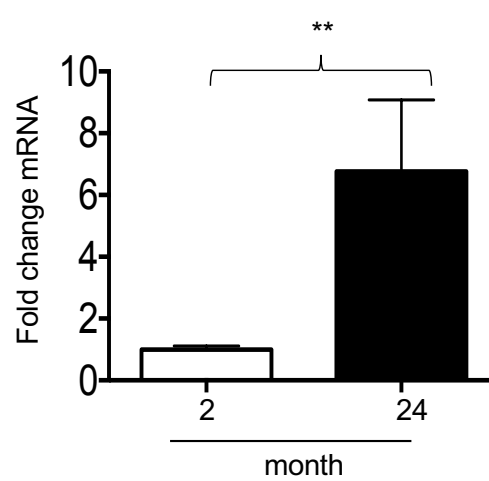
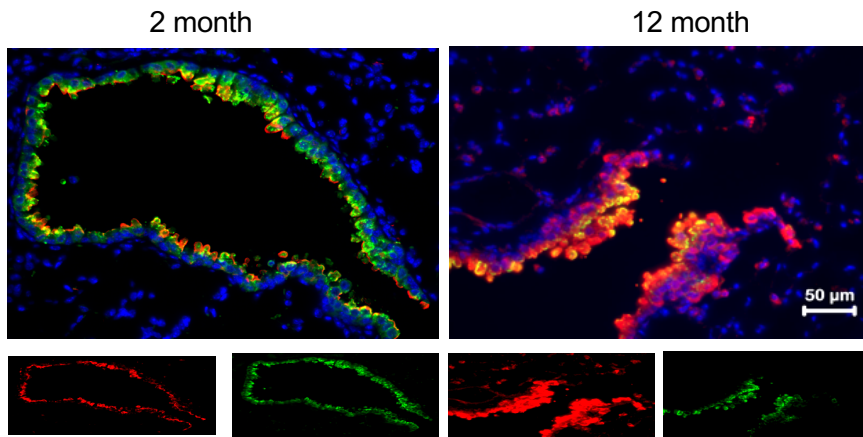
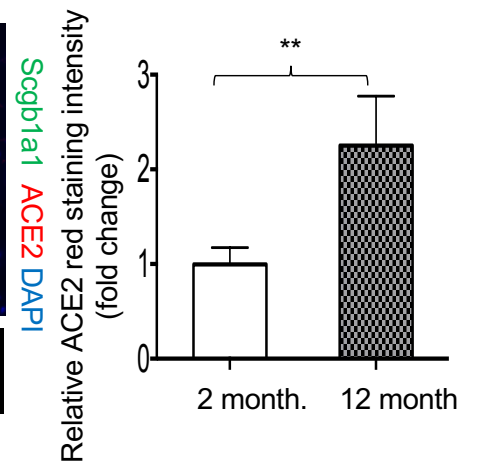


Figure 1

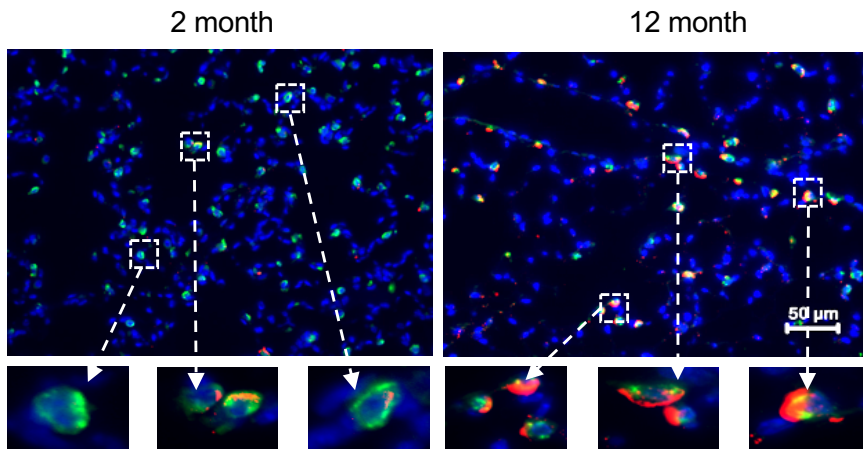
**a**



**b**



**c**



**d**

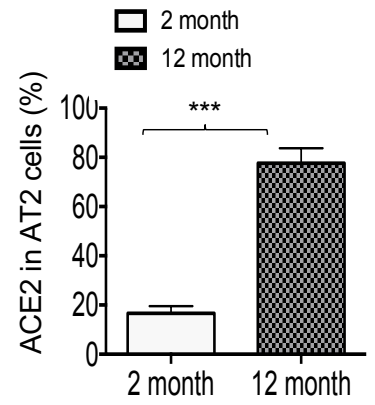


Figure 2

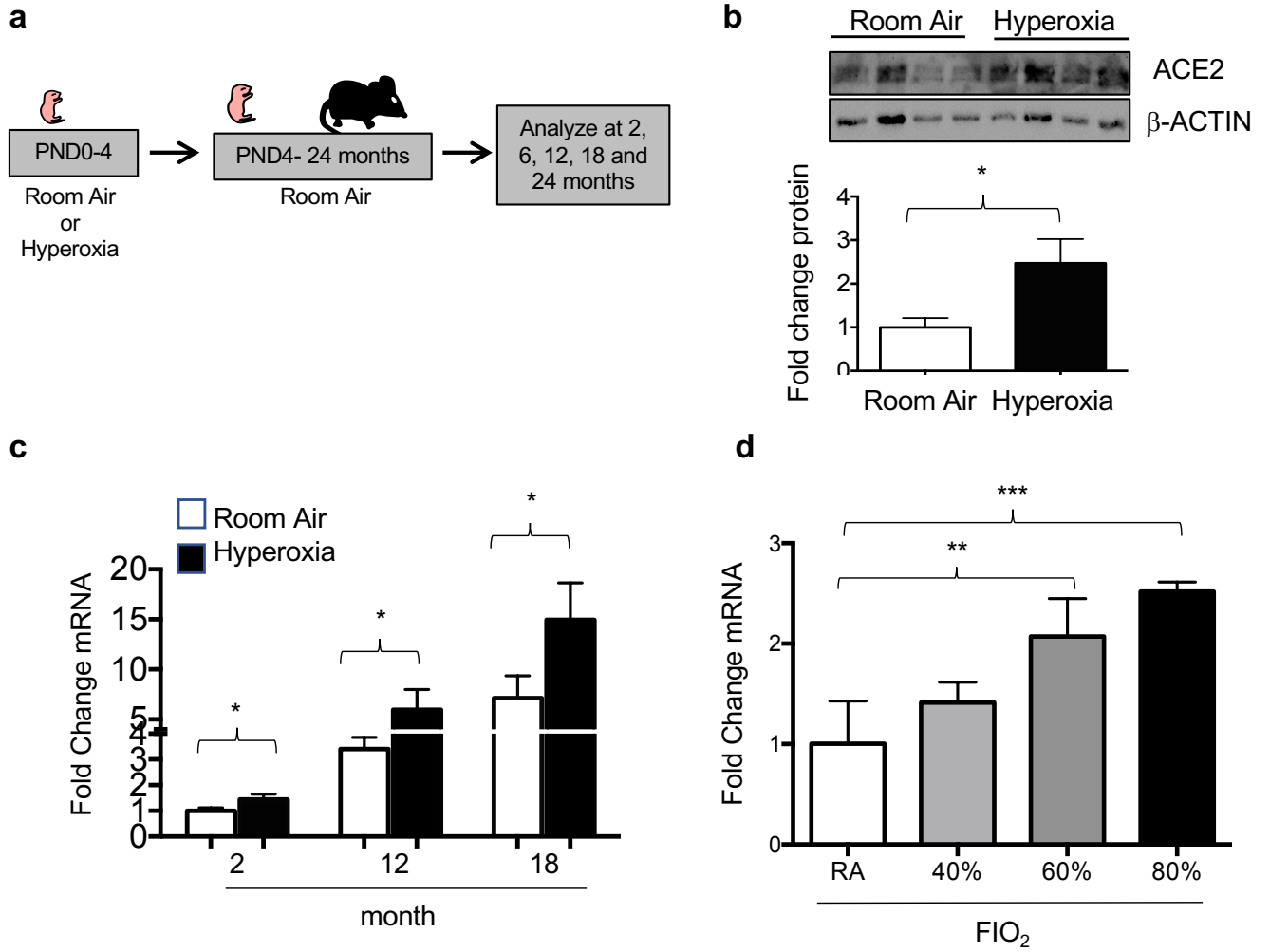


Figure 3

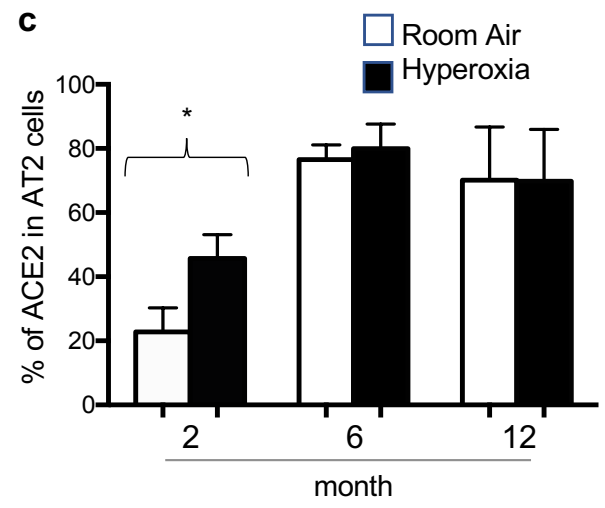
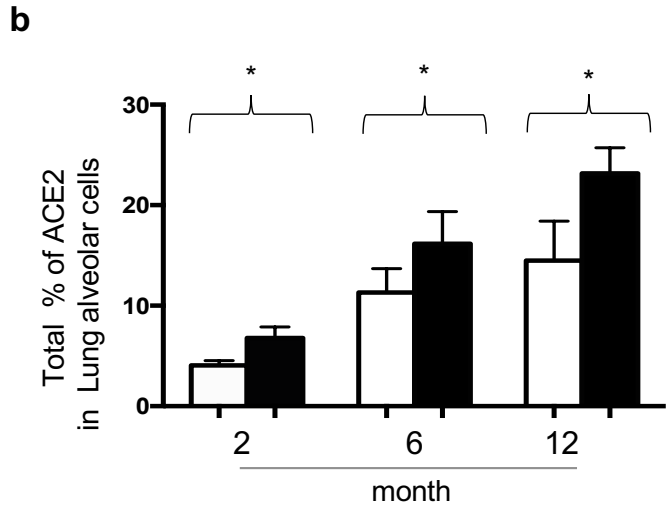
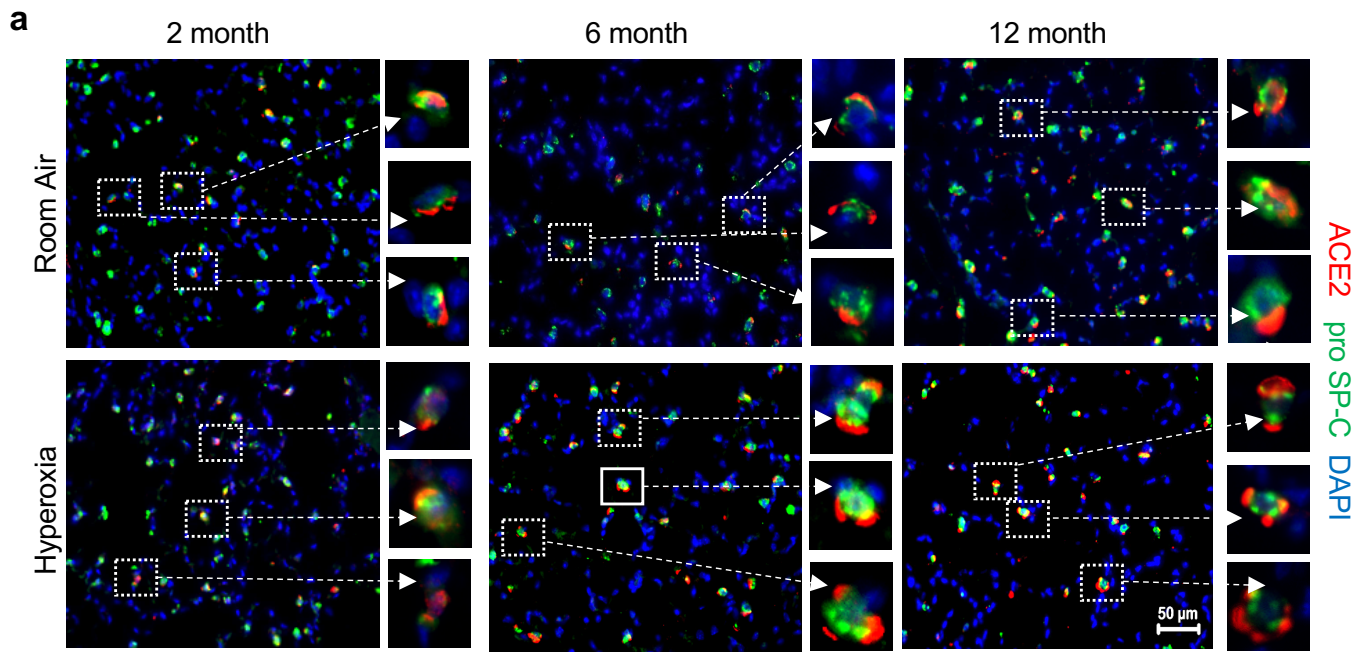


Figure 4

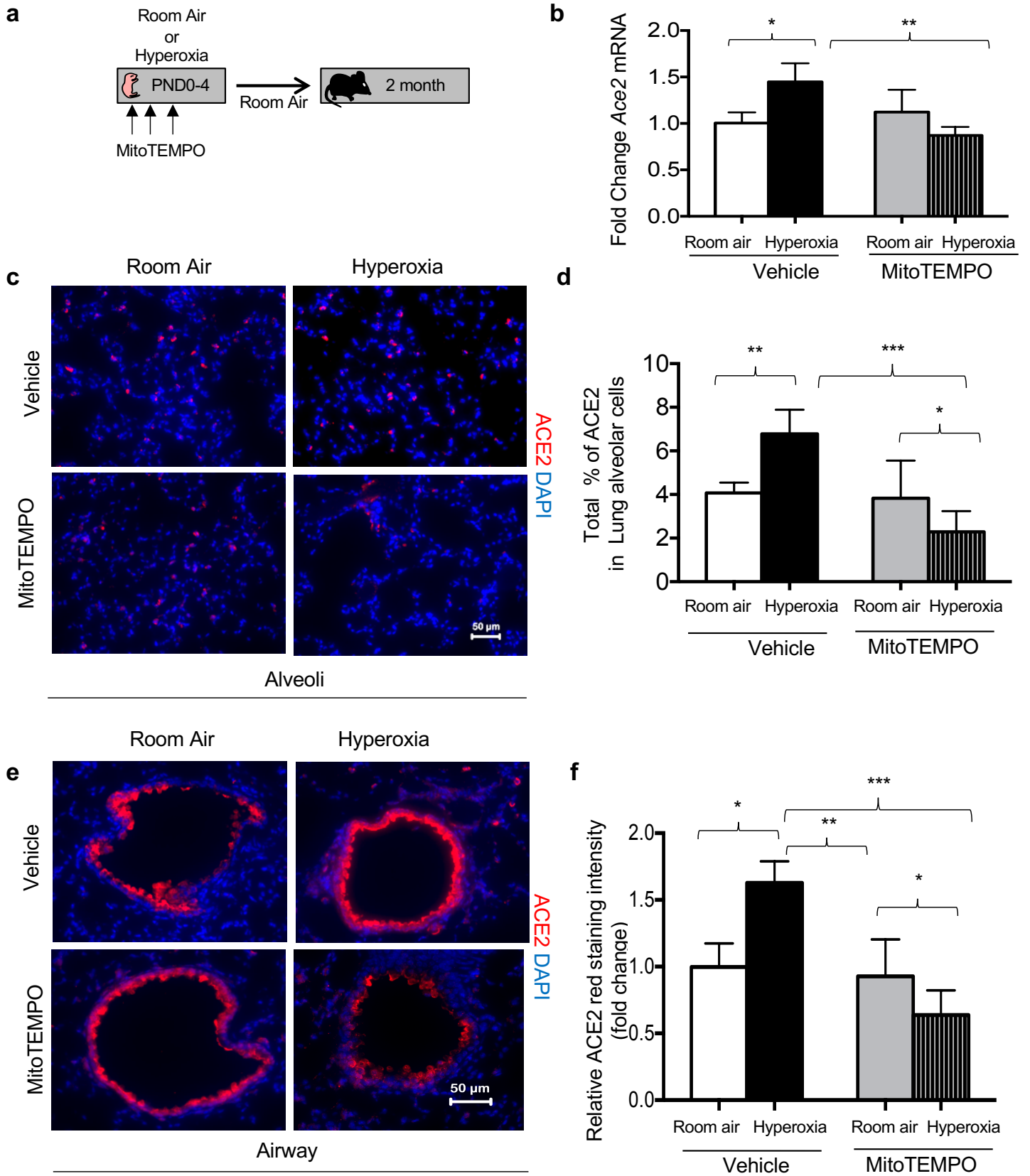


Figure 5

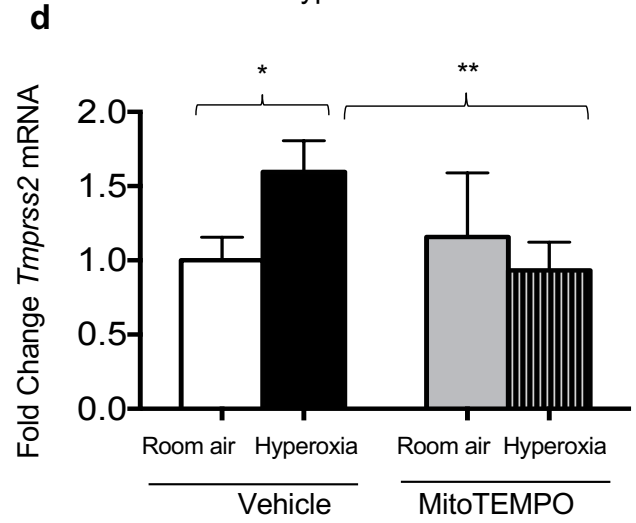
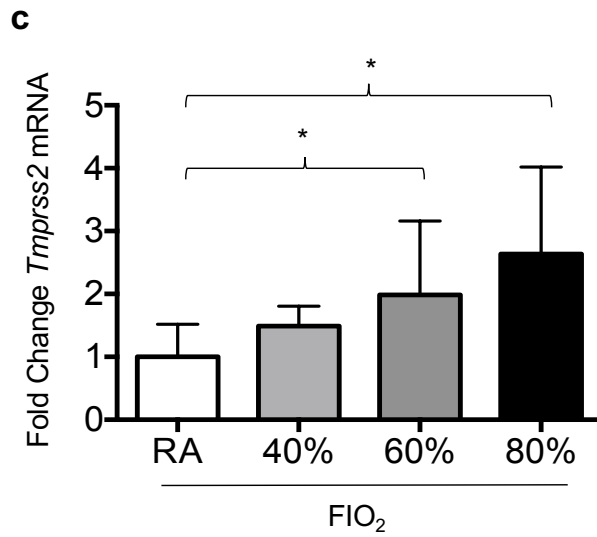
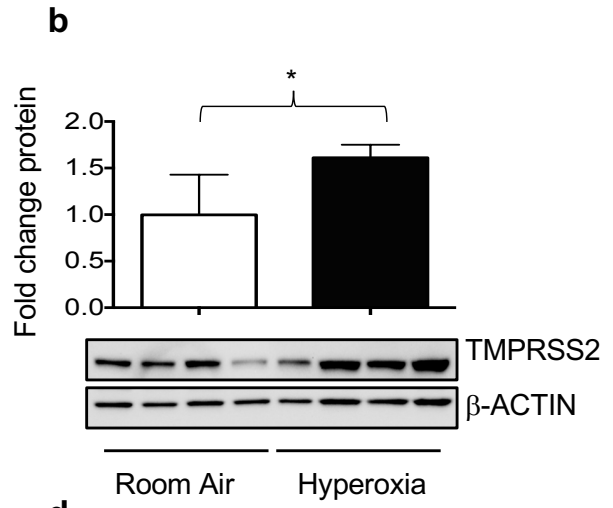
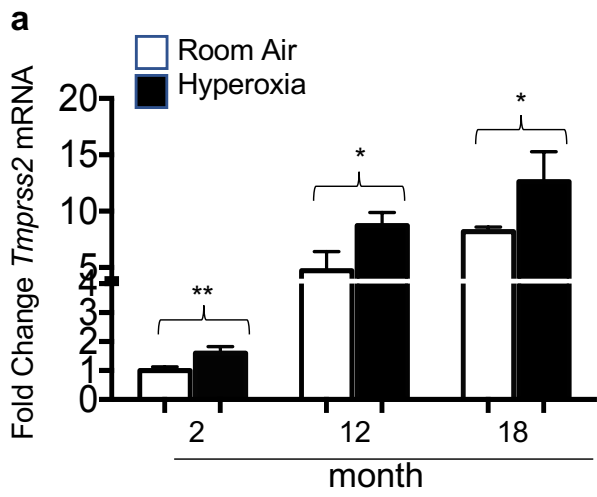


Figure 6